A functional dynamics approach to modelling of glycolysis

F. Hynne, S. Danø and P.G. Sørensen

The access to ever increasing computer power as well as the availability of huge amounts of raw data from high-throughput experimental techniques in genomics and proteomics have renewed the interests in the modelling of biosystems. The dream is *in silicio* biology where computer models have become so sophisticated that answers to biological relevant questions can equally well – but with much less effort – be given by the computer as by the cell.

A number of current research projects have very ambitious goals. Some intend to model huge and complex biosystems quantitatively, while others aim at reconstructing the reaction network of an entire cell from gene expression data. We, however, have a more humble goal in the research presented here. In an effort to take biochemical modelling as far as possible in terms of realism, we have limited ourselves to the very well defined system of glycolysis in yeast cells showing metabolic oscillations [1]. For this particular experimental system there is a host of data avaliable describing both enzymatic, metabolic and dynamic properties. The aim of our modelling is to achieve quantitative agreement with all available experimental findings for this particular system.

If the ultimate goal is *in silicio* biology for an entire cell, then why is it interesting to model a small fraction of yeast metabolism? The answer has three parts.

One is that glycolysis in a yeast cell is one of the simplest mechanisms by which a cell can remain alive, so that the faithfullnes which can be reached modelling this system sets an upper limit of what can be hoped for by complete cell modelling in more complex situations.

The modelling of this system using conventional methods is still a formidable task. It is of primary importance that we have developed a new metod for the optimization of biochemical models which reduces the size of the parameter fitting problem by exploiting constraints imposed by stochiometry and mass flow balances. Also the computational efficacy is increased by including system dynamics in the fitting. We expect that the method presented here is relevant in a much broader context than yeast glycolysis. Still, the method cannot handle the entire cell if realistic modelling in terms of biochemical reactions is intended. The paramount problem is that the size of the parameter space that needs to be searched

Received by the editors January 30, 2002.

in order to find a parameter set which agree with experiments, grows exponentially with the number of unknown parameters. As a consequence, even the fastest computers will never be able to solve much larger systems. Therefore, the availability of expression profiles for the around 6000 genes in *Saccharomyces cerevisiae* does not imply that one has ample data to model its genetic regulation. It merely reflects the fact that the entire yeast cell is an extremely complicated entity.

From a more philosophical point of view, one could argue that there is a context hierarchy in biology: function (dynamics), energy and mass flow (metabolism), reactions (enzymes), and templates (genes). This implies that metabolism is closer to the biological function than the genome, and that even though the genes are important, they do not constitute a blueprint for cellular function. Therefore, it might be more fruitful to model metabolism than genomics, especially because the complexity of the metabolome is much lower than that of the genome (600 metabolites vs. 6000 genes in *Saccharomyces cerevisiae*), but also because the problem becomes more tractable by exploiting physical and chemical constraints on metabolism.

The work described here involves a new fitting procedure, new ways of combining mechanistic and dynamical data, as well as a lot of biochemical and experimental considerations and comparisons. With the space avaliable, we cannot possibly account for the details of the rigorous mathematics underlying the fitting procedure, nor can we give a detailed account of the use of experimental data. For such information, the reader should consult Ref. [2] which is an in-depth description of the present work.

1. The biological system

The system which we intend to model is yeast cells in an open flow reactor (a CSTR) with constant inflow of glucose, cyanide and cell suspension and outflow of surplus liquid. This setup allows us to control the state of the cells precisely by controlling the rates of the various inflows, and the particular operating point which we model corresponds to the onset of sustained oscillations as the inflow of glucose is increased. By a combination of such manipulations and the use of special perturbation experiments we have characterized the onset of oscillations at the operating point as the emergence of almost simultaneous supercritical Hopf bifurcations in each of the yeast cells [3, 2]. The significance of this observation is that the yeast cell dynamics follow a simple equation which describes the behaviour of systems close to this type of bifurcation. The close correspondence between a solution to this equation – the Stuart-Landau equation – and the cell behavior is illustrated by Fig. 1, where the Stuart-Landau equation is fitted to two perturbation experiments, where either glucose or acetaldehyde is added in preciesely the unique amount and unique phase that causes a momentary quenching of the oscillations. This characterization of the dynamics is a big advantage for the parameter fitting, since it provides us with a tractable mathematical framework for

the comparison between the dynamics of the model and the dynamics of the yeast cells.

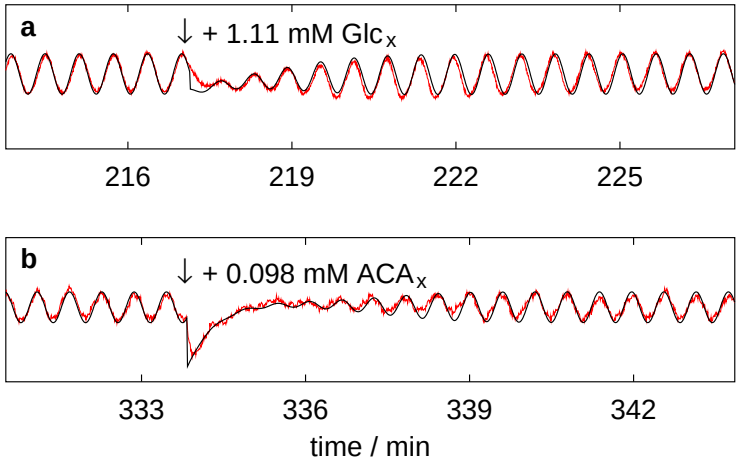

FIGURE 1. Fit of a Stuart-Landau equation (black curves) to two different quenching experiments (red curves), where the instantaneous addition of glucose (a) and acetaldehyde (b) causes a momentary quenching of the oscillations. Experimental data from [3], see Ref. [4] for details of the fitting.

Furthermore, the yeast cells are known to be strongly coupled [5, 6, 7], so we can assume that the behaviour of a single typical yeast cell can be inferred from that of the entire population. Obviously, this is a big advantage during the parameter fitting.

The experimental design helps to reduce the complexity of the biological system considerably. The cells in the experiments are starved beforehand, so they only have a limited amount of amino acids avaliable for protein synthesis. This ensures that the cells are non-growing, and that the enzyme composition of the yeast cells does not change significantly in the rather short time course of the experiments. Furthermore, the presence of cyanide effectively blocks the respiratory part of the metabolism, so we are left with glycolysis and fermentation plus a branch for glycerol production and a branch for glycogen buildup. This reaction network is shown in Fig. 2.

Apart from working with a well defined system, it is of utmost importance to have as much experimental data avaliable as possible. As described in Ref. [2], one can combine the CSTR experiments with experiments performed on the oscillating transients observed when first a glucose pulse and then a cyanide pulse is added to a suspension of yeast cells (batch experiments; Refs. [8, 7, 9]). The combined data

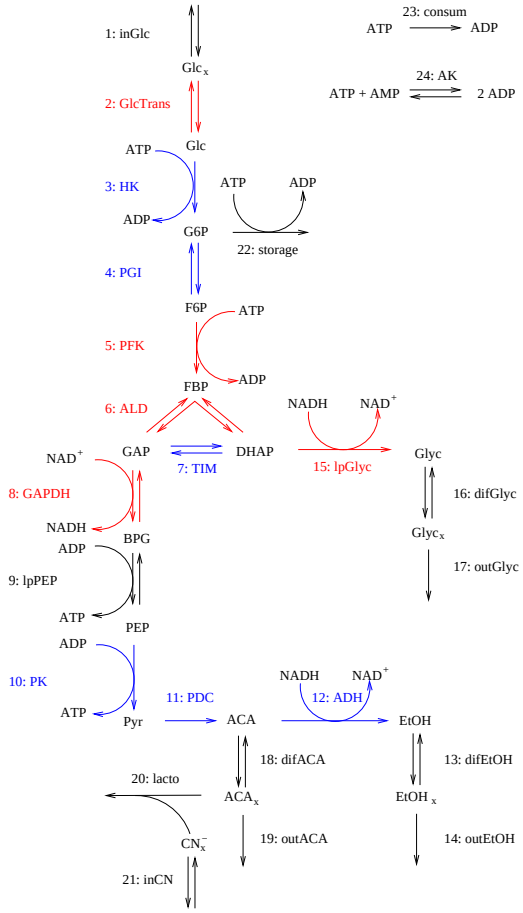

FIGURE 2. The reaction network of the model. Rate equations for the reactions with red colour coding are given in Table 1, blue colour coding indicates that the reaction is modelled with a standard Michaelis-Menten like rate equation, and black colour coding indicates that the reaction is modelled with mass action kinetics. Reactions 2,13,16, and 18 are membrane transport reactions and reactions 1,14,17,19, and 21 are in/out flows of the CSTR.

set has data on the period of oscillations, on 13 metabolite concentrations, on the glycolytic flux and on its branching ratios. We also have measurements of 9 phases and 13 amplitudes of metabolites during the oscillations, data on the mechanical operating conditions of the CSTR and the precise location of the Hopf bifurcation, as well as the period of oscillations and data from the quenching experiments. We

also have *in vitro* data on 24 enzyme kinetic parameters. All of these data were included in the parameter fitting of the model as described in the following section.

2. Development of the model

The first thing to consider when developing a model is the type of equations. It is by far most convenient to work with a set of ordinary differential equations, but that might not always give an adequate description of the system. There are two issues to consider: Is the number of molecules big enough, and is the system spatially homogeneous?

In metabolism one is generally in the milimolar range of concentrations, so within a typical yeast cell of say 6 μm diameter one will find $N \approx 10^7$ for each of the metabolites. Stochastic fluctuations are on the order of $\sqrt{N} \approx 3 \cdot 10^3$ which is less than $1‰$ of N. However, one might run into trouble when modelling other cellular systems, notably the regulatory network of the genome.

Intracellular spatial homogeneity is ensured by diffusion if the volume of the cell is small enough. That is, the characteristic time for diffusive mixing in the spatial compartment should be less than the characteristic time of the dynamics in question. Again, for a typical yeast cell we have $t_{\mathrm{mix}} \approx \frac{L^2}{\pi^2 D} < 0.1\mathrm{s}$ when the diffusion constant D is taken to a typical value for metabolites in water, $5 \cdot 10^{-6}\mathrm{cm}^2/\mathrm{s}$. This seems small when compared to the 35–40s period of the observed oscillations. Nevertheless, travelling NADH waves have been observed in neutrophiles which are elongated cells with a typical length of 20 μm [10], so in general one cannot rule out the possibility of spatial heterogeneity. Still, the wavelength of the NADH waves observed in that study is so large that they would not fit in a yeast cell. Consequently, we will assume that the yeast cells are spatially homogeneous.

We will assume that the enzyme activity is the same for all experiments used in the parameter fitting. Note that this only makes sense if the experimental values are obtained for identical cells which are truly in the same proteomic state and that this state remains constant during the experiments. Closer inspection shows that the cells are not completely identical but have for example a size distribution. If the distribution in properties is narrow the dynamics is almost identical with the dynamics for a system with identical cells. A discussion of this synchronization problem can be found in Ref. [4]. The time constancy of cell properties is only approximately valid in the batch experiments, but is confirmed for the CSTR through the remarkable long-time stability of the oscillatory amplitude [3].

Since our goal is a quantitatively and biochemically realistic description of the yeast cell experiments, we formulate our model so that direct comparisons between experimental findings and model predictions can be made. The intention is to make the model as simple as possible, but nevertheless the need for comparison with experiments makes it rather detailed with 24 reactions (of which 12 are reversible), 22 metabolites and 59 parameters. (Details of the model can be inferred from Fig. 2 and Table 1 or found in Ref. [2].) Fig. 3 depicts the system described by the model.

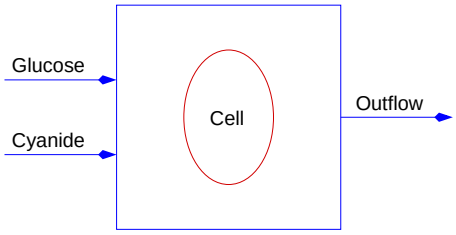

FIGURE 3. Schematic figure of a yeast cell in a CSTR. In the real experiments the reactor contained 1 billion cells. The dynamics of a one-cell reactor is identical to the dynamics of a many-cell reactor provided the state af the cells are identical, and the flow rate and volume is increased in proportion with the number of cells.

In the model we assume that the functional forms of the rate expressions are known for each enzyme for example from *in vitro* studies. What remains to be chosen is the values of the kinetic parameters in the rate expressions. The kinetic parameters is a collection of rate constants, maximum velocities, Michaelis-Menten parameters and other parameters. Most of these constants have been determined in *in vitro* experiments on isolated enzymes. We have, however, no guarantee that the *in vitro* values are applicable when the enzymes are embedded in a living cell. The maximum velocities for the enzymes in the living cell depend on the enzyme activities and these values are largely unknown.

In principle, we want to test all possible parameter combinations and pick the one which gives the best match with experiments. However, this is not possible since the number of possible parameter combinations is astronomical. So, we need to decrease the size of the parameter fitting task. The basic observation, which allows us to do this, is the fact that the behaviour of a chemical reaction system is determined by the stochiometry of its reactions and the kinetics of each of these. The connection between stochiometry and concentrations is given by

$$\frac{\mathrm{d}c_s}{\mathrm{d}t} = \sum_r \nu_{sr} v_r \qquad \text{or in matrix notation} \qquad \dot{\mathbf{c}} = \boldsymbol{\nu} \cdot \mathbf{v} \tag{1}$$

where c_s is the concentration of the metabolite s, v_r is the velocity of reaction r, and ν_{sr} is the stochiometric coefficient of metabolite s in reaction r. This equation simply states that the total change in the concentration of a given metabolite is the sum of the changes caused by the individual reactions, and that each of these contributions is given by the velocity of that reaction multiplied by the stochiometric coefficient for that reaction. In matrix notation the time derivatives of the concentrations are collected in a vector $\dot{\mathbf{c}}$, the reaction velocities are collected in a vector $\mathbf{v}$, and the stochiometric coefficients are collected in a matrix $\boldsymbol{\nu}$. Our first trick is to work only with the stationary states of the reaction system. Since we want to model the yeast cell system at the point where the stationary state

r	Rate Equation (v_r)
2:	$v_{\rightarrow} = \dfrac{V_{2\mathrm{m}}\frac{[\mathrm{Glc_x}]}{K_{2\mathrm{Glc}}}}{1+\frac{[\mathrm{Glc_x}]}{K_{2\mathrm{Glc}}}+\frac{P_2\frac{[\mathrm{Glc_x}]}{K_{2\mathrm{Glc}}}+1}{P_2\frac{[\mathrm{Glc}]}{K_{2\mathrm{Glc}}}+1}\left(1+\frac{[\mathrm{Glc}]}{K_{2\mathrm{Glc}}}+\frac{[\mathrm{G6P}]}{K_{2\mathrm{IG6P}}}+\frac{[\mathrm{Glc}][\mathrm{G6P}]}{K_{2\mathrm{Glc}}K_{2\mathrm{IIG6P}}}\right)}$
	$v_{\leftarrow} = \dfrac{V_{2\mathrm{m}}\frac{[\mathrm{Glc}]}{K_{2\mathrm{Glc}}}}{1+\frac{[\mathrm{Glc}]}{K_{2\mathrm{Glc}}}+\frac{P_2\frac{[\mathrm{Glc}]}{K_{2\mathrm{Glc}}}+1}{P_2\frac{[\mathrm{Glc_x}]}{K_{2\mathrm{Glc}}}+1}\left(1+\frac{[\mathrm{Glc_x}]}{K_{2\mathrm{Glc}}}\right)+\frac{[\mathrm{G6P}]}{K_{2\mathrm{IG6P}}}+\frac{[\mathrm{Glc}][\mathrm{G6P}]}{K_{2\mathrm{Glc}}K_{2\mathrm{IIG6P}}}}$
5:	$v_{\rightarrow} = \dfrac{V_{5\mathrm{m}}[\mathrm{F6P}]^2}{K_5\left(1+\kappa_5\frac{[\mathrm{ATP}]^2}{[\mathrm{AMP}]^2}\right)+[\mathrm{F6P}]^2}$
6:	$v_{\rightarrow} = \dfrac{V_{6\mathrm{f}}[\mathrm{FBP}]}{K_{6\mathrm{FBP}}+[\mathrm{FBP}]+\frac{[\mathrm{GAP}]K_{6\mathrm{DHAP}}V_{6\mathrm{f}}}{K_{6\mathrm{eq}}V_{6\mathrm{r}}}+\frac{[\mathrm{DHAP}]K_{6\mathrm{GAP}}V_{6\mathrm{f}}}{K_{6\mathrm{eq}}V_{6\mathrm{r}}}+\frac{[\mathrm{FBP}][\mathrm{GAP}]}{K_{6\mathrm{IGAP}}}+\frac{[\mathrm{GAP}][\mathrm{DHAP}]V_{6\mathrm{f}}}{K_{6\mathrm{eq}}V_{6\mathrm{r}}}}$
	$v_{\leftarrow} = \dfrac{V_{6\mathrm{f}}\frac{[\mathrm{GAP}][\mathrm{DHAP}]}{K_{6\mathrm{eq}}}}{K_{6\mathrm{FBP}}+[\mathrm{FBP}]+\frac{[\mathrm{GAP}]K_{6\mathrm{DHAP}}V_{6\mathrm{f}}}{K_{6\mathrm{eq}}V_{6\mathrm{r}}}+\frac{[\mathrm{DHAP}]K_{6\mathrm{GAP}}V_{6\mathrm{f}}}{K_{6\mathrm{eq}}V_{6\mathrm{r}}}+\frac{[\mathrm{FBP}][\mathrm{GAP}]}{K_{6\mathrm{IGAP}}}+\frac{[\mathrm{GAP}][\mathrm{DHAP}]V_{6\mathrm{f}}}{K_{6\mathrm{eq}}V_{6\mathrm{r}}}}$
8:	$v_{\rightarrow} = \dfrac{V_{8\mathrm{m}}[\mathrm{GAP}][\mathrm{NAD^+}]}{K_{8\mathrm{GAP}}K_{8\mathrm{NAD}}\left(1+\frac{[\mathrm{GAP}]}{K_{8\mathrm{GAP}}}+\frac{[\mathrm{BPG}]}{K_{8\mathrm{BPG}}}\right)\left(1+\frac{[\mathrm{NAD^+}]}{K_{8\mathrm{NAD}}}+\frac{[\mathrm{NADH}]}{K_{8\mathrm{NADH}}}\right)}$
	$v_{\leftarrow} = \dfrac{V_{8\mathrm{m}}\frac{[\mathrm{BPG}][\mathrm{NADH}]}{K_{8\mathrm{eq}}}}{K_{8\mathrm{GAP}}K_{8\mathrm{NAD}}\left(1+\frac{[\mathrm{GAP}]}{K_{8\mathrm{GAP}}}+\frac{[\mathrm{BPG}]}{K_{8\mathrm{BPG}}}\right)\left(1+\frac{[\mathrm{NAD^+}]}{K_{8\mathrm{NAD}}}+\frac{[\mathrm{NADH}]}{K_{8\mathrm{NADH}}}\right)}$
15:	$v_{\rightarrow} = \dfrac{V_{15\mathrm{m}}[\mathrm{DHAP}]}{K_{15\mathrm{DHAP}}\left(1+\frac{K_{15\mathrm{INADH}}}{[\mathrm{NADH}]}\left(1+\frac{[\mathrm{NAD^+}]}{K_{15\mathrm{INAD}}}\right)\right)+[\mathrm{DHAP}]\left(1+\frac{K_{15\mathrm{NADH}}}{[\mathrm{NADH}]}\left(1+\frac{[\mathrm{NAD^+}]}{K_{15\mathrm{INAD}}}\right)\right)}$

TABLE 1. Selected rate equations of the model. The remaining reactions are modelled either by standard Michaelis-Menten like rate equations or by mass action kinetics as indicated by the colour coding in Fig. 2.

becomes unstable and oscillations emerge, this is a fully valid description of the experimental system. For stationary states we have $\dot{\mathbf{c}} = \mathbf{0}$, so these states can be found from Eq. 1 as the null space of $\boldsymbol{\nu}$ which is the space of all vectors $\mathbf{v}$ for which $\boldsymbol{\nu} \cdot \mathbf{v} = \mathbf{0}$. Geometrically, the relevant part of velocity space is a polygonal cone (colloquially: a pyramid of infinite height) extending from origo, and it is generally of smaller dimension than the velocity space. The cone is known as the current cone, and the velocity vectors defining the edges of the cone are known as the extreme currents. These concepts are illustrated in Fig. 4.

Chemical kinetics must also be included in the description in order to make it complete. The rate of a chemical reaction r can generally be written as

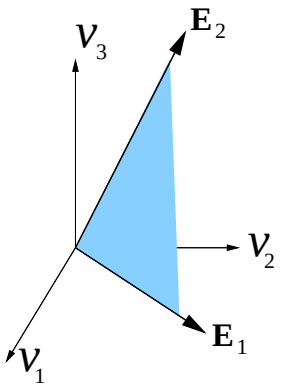

FIGURE 4. Sketch of a two-dimensional current cone in a three-dimensional velocity space. v_1, v_2 and v_3 are the velocities of three reactions, and $\mathbf{E}_1$ and $\mathbf{E}_2$ are the extreme currents defining the edges of the current cone which is shaded light blue. These edges appear because all velocities are non negative. In this fictitious three-reaction system, stationary states are only found on the two-dimensional current cone.

$$v_r = \mathrm{V}_r g_r(\mathbf{c}, \mathbf{K}_r) \tag{2}$$

where V_r is the "velocity parameter" of the reaction, $\mathbf{c}$ is a vector containing the concentrations of the metabolites of the reaction system, and $\mathbf{K}_r$ is a vector containing the "intrinsic parameters" of the reaction (*i.e.* all the remaining parameters after the velocity parameter has been factored out). Consider, for example, the rate equation of reaction 5 (Table 1). Here $\mathrm{V}_5 = \mathrm{V}_{5\mathrm{m}}$, $g_5 = [\mathrm{F6P}]^2 / \left(K_5 \left(1 + \kappa_5 \frac{[\mathrm{ATP}]^2}{[\mathrm{AMP}]^2}\right) + [\mathrm{F6P}]^2\right)$, and $\mathbf{K}_5$ is the set of K_5 and κ_5. The splitting of the parameters into velocity parameters and intrinsic parameters makes it straight forward to take advantage of the possibility to calculate stationary velocities from the stochiometry of the reaction system. We pick a set of stationary velocities $\mathbf{v}$, a set of intrinsic parameters $\mathbf{K}_r$ for each of the reactions, and any set of concentrations $\mathbf{c}$ which we want to become stationary concentrations of the model. From these we can now calculate the intrinsic parameters of all the reactions as $\mathrm{V}_r = v_r / g_r(\mathbf{c}, \mathbf{K}_r)$. This way we fit one parameter *per reaction* by invoking the stationarity condition, and we also obtain a model which – by construction – has a stationary state with the experimentally determined concentrations. This is achieved solely through algebraic operations, which are extremely efficient when compared to the usual fitting procedures involving numeric integration of the kinetic equations or repeated Newton iterations of the rate expressions describing the reaction system. For biochemical systems, the direct calculation of the velocity

parameters is very convenient, since these parameters are inherently difficult to measure.

When considering only stationary states, one might think that the dynamical properties of the system cannot be included in the parameter fitting. This is, however, not the case. The dynamics near a stationary state can be described quite accurately by a linearization of the kinetics around this state. Furthermore, by choosing the operating point for the parameter fitting as the point where the stationary state loses stability and the oscillations emerge, we have in a sense a stationary state and an oscillatory state at the same time. So, in the course of the parameter fitting we calculate the frequency of the oscillations, the relative amplitudes of the different metabolites, their relative phases, and the parameters characterizing the quenching responses show in Fig. 1 from the linearized kinetics of the stationary state. These system properties are then included in the model validation. Again, the calculations involved are algebraic operations, so they do not consume excessive amounts of computer power as in the classical methods based on integration of the kinetic equations. (Technically, the dynamical properties are calculated from the eigenvalues and the left and right eigenvectors of the Jacobian matrix.)

With the procedure described above, we can evaluate the agreement with experiments for a given set of parameters in an extremely efficient way. Therefore, we can easily scan several million parameter combinations. Furthermore, we have a rather large collection of experimental data on the system as described at the end of Section 1. The data on the size of the glycolytic flux and its branching ratios together with the operating conditions of the CSTR are used to pick realistic stationary velocities, which are then plugged into Eq. 2 along with the known metabolite concentrations and the known enzyme kinetic parameters. These values are then supplemented with values for the unknown enzyme kinetic parameters and values for the metabolite concentrations which have not been determined experimentally. The data describing the relative phases and amplitudes of the metabolites during the oscillations, the frequency of oscillations, the special perturbation experiments of Fig. 1 as well as the type and direction of the bifurcation are used in the model validation. Even with the procedure presented here, it is impossible to do a full scan of all relevant parameter combinations. But it is possible to try out a large number of parameter combinations, so with suitable human guidance it was possible to arrive at a model which is biochemically realistic and in quantitative agreement with almost all experimental observations.

3. Results of the optimization

The optimized parameter set was selected after an evaluation of more than 100 million parameter combinations. An in depth discussion of the achieved results can be found in Ref. [2]. Only the main points are summarized here. The values of the parameters for the operating conditions of the reactor such as the glycolytic

flux were in complete agreement with the actual operating conditions. We also obtained exact agreement with experimental estimates for the branching coefficients for fermentation, glycerol production, lactonitril formation and glycogen buildup. Exact agreement between the model and the experiments was also obtained for the location and type of the bifurcation, just as the period of oscillations was fixed to the measured value of 37.5s. Table 2 shows a comparison of model values with experimental values for metabolite concentrations c_s, oscillation amplitudes a_s, oscillation phases θ_s, quenching concentrations q_s, and quenching phases ϕ_s.

	c_s/mM	a_s/a_{NADH}	θ_s/deg	$q_s/q_{\mathrm{ACA_x}}$	ϕ_s/deg
$\mathrm{Glc_x}$	1.55 (1.6)	0.013	135	5.3 (11)	355 (4)
Glc	0.57	1.83	12	18	81
G6P	4.2 (4.1)	15.8 (21)	190 (260)	1.7	67
F6P	0.49 (0.5)	2.16 (2.7)	178 (250)	1.7	72
FBP	4.64 (5.1)	22.2 (26)	32 (70)	4.4	218
GAP	0.115 (0.12)	0.295 (0.04)	30	7.0	255
DHAP	2.95 (2.5)	6.97 (0.5)	38	7.9	195
BPG	0.0003 (n.d)	0.002	136	0.53	287
PEP	0.04 (0.04)	0.023 (0.07)	18	1.1	286
Pyr	8.7 (8.7)	4.06 (7)	79	125	180
ACA	1.48	0.894	196	2.5	268
$\mathrm{EtOH_x}$	16.5	0.035	114	∞ (n.p)	undef
EtOH	19.2	1.22	26	∞	undef
Glyc	4.2	1.68	98	∞	undef
$\mathrm{Glyc_x}$	1.68	0.005	188	∞ (n.p)	undef
$\mathrm{ACA_x}$	1.29	0.037 (0.3)	284 (200)	1 (1)	181 (172)
$\mathrm{CN_x^-}$	5.2	5×10^{-5}	193	2400 (n.p)	271
ATP	2.1 (2.1)	10.8 (8)	139 (180)	0.50	289
ADP	1.5 (1.5)	6.32 (9.4)	319 (0)	1.0	290
AMP	0.33 (0.33)	4.5 (3.6)	319 (0)		
NADH	0.33 (0.33)	1 (1)	0 (0)	0.68	106
$\mathrm{NAD^+}$	0.65 (0.65)	1 (0.6)	180 (180)		

TABLE 2. Comparison of model results with experimental results related to metabolites: concentrations c_s of metabolites s, amplitudes of oscillations a_s in units of the NADH amplitude, phases of oscillations θ_s relative to the phase of NADH, quenching concentrations q_s in units of the $\mathrm{ACA_x}$ quenching concentration, and quenching phases ϕ_s relative to the phase of NADH. Experimental results are quoted in parenthesis. The origin of the experimental results are described in Ref. [2]. n.d.: not detectable. n.p.: quenching was attempted but was not possible. This corresponds to a large value of $q_s/q_{\mathrm{ACA_x}}$.

All the stationary concentrations agrees quite well with the experimental determinations. The same is true for most of the amplitudes of the oscillations. Noteworthy execptions are the amplitude of GAP and DHAP. The fit of the phases are less satisfactory. Note the good agreement for the quenching amplitude ratio and quenching phases of Glc_x and ACA_x. The quenching additions are made to the extracellular medium. Together with the fast cellular response to an instantaneous perturbation shown in Fig.1 they demonstrate that the transport of Glc and ACA through the membrane is fast compared with the period of oscillation. Perhaps the most interesting result from the parameter fitting is that we have obtained a determination of the activities for the glycolytic enzymes inside a living cell based on experimental measurements. More tables with comparisons are given in Ref. [2]. The data in one of these tables demonstrates that the values for the Michaelis-Menten constants for the selected parameter point agrees remakably well with litterature values. The model also compares well with experimental behavior at other operating points.

4. Discussion and perspectives

We have presented a powerful, general method, based on functional dynamics, for fitting of kinetic parameters of a model for an entire pathway in a living cell to experimental data. All experiments are made at a fixed stationary state under experimental conditions where it can be assumed that the enzyme activities are constant. Rate constants and maximum velocities are determined by simple algebra without numeric integration of the kinetic equations. The model agrees with almost all experimental observations and data for *Saccharomyces cerevisiae* at an operating point where metabolic oscillations have just emerged. Basically, the method can be used for other systems at a stationary state where substantial experimental material for stationary and dynamic properties is available. The use of measured dynamical properties for small amplitude deviations from the stationary state is a new and important addition to the efficacy of the fitting procedure. Fundamentally the method does not depend on the existence of small amplitude oscillations. By using the method on stationary states of different environmental conditions and for mutant organisms quantitative information can be obtained about the metabolome which is at the heart of biological function.

5. Acknowledgements

We thank the Danish Research Agency for funding the Center for Chaos and Turbulence Studies (CATS) and the Functional Dynamics initiative.

References

[1] B. Chance, R. W. Estabrook, and A. Ghosh. Damped Sinusoidal Oscillations of Cytoplasmic Reduced Pyridine Nucleotide in Yeast Cells. Biochemistry, **51**:1244–1251 (1964)

[2] F. Hynne, S. Danø, and P. G. Sørensen. Full-scale model of glycolysis in *Saccharomyces cerevisiae*. Biophys. Chem., **94**:121–163 (2001)

[3] S. Danø, P. G. Sørensen, and F. Hynne. Sustained oscillations in living cells. Nature, **402**:320–322 (1999)

[4] S. Danø, F. Hynne, S. De Monte, F. d'Ovidio, P. G. Sørensen, and H. Westerhoff. Synchronization of glycolytic oscillations in a yeast cell population. Faraday Discuss., **120**:261–276 (2001)

[5] E. K. Pye. Biochemical mechanisms underlying the metabolic oscillations in yeast. Can. J. Botany, **47**:271–285 (1969)

[6] A. K. Ghosh, B. Chance, and E. K. Pye. Metabolic Coupling and Synchronization of NADH Oscillations in Yeast Cell Populations. Arch. Biochem. Biophys., **145**:319–331 (1971)

[7] P. Richard, B. M. Bakker, B. Teusink, K. van Dam, and H. V. Westerhoff. Acetaldehyde mediates the synchronization of sustained glycolytic oscillations in populations of yeast cells. Eur. J. Biochem., **235**:238–241 (1996)

[8] P. Richard, J. A. Diderich, B. M. Bakker, B. Teusink, K. van Dam, and H. V. Westerhoff. Yeast cells with a specific cellular make-up and an environment that removes acetaldehyde are prone to sustained glycolytic oscillations. FEBS Letters, **341**:223–226 (1994)

[9] P. Richard, B. Teusink, M. B. Hemker, K. van Dam, and H. V. Westerhoff. Sustained Oscillations in Free-energy State and Hexose Phosphates in Yeast. Yeast, **12**:731–740 (1996)

[10] H. R. Petty, R. G. Worth, and A. L. Kinzelskii. Imaging Sustained Dissipative Patterns in the Metabolism of Individual Living Cells. Phys. Rev. Lett., **84**:2754–2757 (2000)